

Citation for published version:

Ding, R, Zhang, J, Xu, B, Cheng, M & Pan, M 2019, 'Energy Efficiency Improvement of Heavy-Load Mobile Hydraulic Manipulator with Electronically Tunable Operating Modes', *Energy Conversion and Management*, vol. 188, pp. 447-461. <https://doi.org/10.1016/j.enconman.2019.03.023>

DOI:

[10.1016/j.enconman.2019.03.023](https://doi.org/10.1016/j.enconman.2019.03.023)

Publication date:

2019

Document Version

Peer reviewed version

[Link to publication](#)

Publisher Rights

CC BY-NC-ND

University of Bath

Alternative formats

If you require this document in an alternative format, please contact:
openaccess@bath.ac.uk

General rights

Copyright and moral rights for the publications made accessible in the public portal are retained by the authors and/or other copyright owners and it is a condition of accessing publications that users recognise and abide by the legal requirements associated with these rights.

Take down policy

If you believe that this document breaches copyright please contact us providing details, and we will remove access to the work immediately and investigate your claim.

Energy Efficiency Improvement of Heavy-Load Mobile Hydraulic Manipulator with Electronically Tunable Operating Modes

Ruqi Ding^a, Junhui Zhang^{b*}, Bing Xu^b, Min Cheng^{b,c}, Min Pan^d

a. Key Laboratory of Conveyance and Equipment, Ministry of Education, East China Jiaotong University, Nanchang, China

b. State Key Laboratory of Fluid Power and Mechatronic Systems, Zhejiang University, Hangzhou, China

c. College of Mechanical Engineering, Chongqing University, Chongqing, China

d. The Centre for Power Transmission and Motion Control, University of Bath, United Kingdom

Abstract: The conventional hydraulic drive system for a heavy-load mobile manipulator is usually operated under single mode, such that both inlet/outlet and potential energy losses are large to lower the energy efficiency. In this paper, a novel electro-hydraulic drive system is presented to improve energy efficiency. Extended control degrees of freedom are obtained utilizing the independent metering valve and electronic controlled pump. Then, multiple operating modes are carried out pertaining to the cylinder, valve, and pump. To achieve both optimal energy efficiency and precise motion tracking, both multi-mode switching and multi-variable controller are designed to accommodate with time-varying and uncertain load characteristics. As a consequence, the inlet, outlet, and potential energy losses can be decreased simultaneously. The experimental validation is conducted by using a three-joint manipulator in a 2t excavator. A duty cycle of movement including all three actuators and covering full load quadrants is used to evaluate the efficiency improvement. Compared with the conventional load sensing system, the proposed multi-mode switching system using the pump pressure with valve meter-in control mode yields a 25.8% energy-saving ratio. Furthermore, the pump flow with valve meter-out control mode yields a 35.3% energy-saving ratio. Using this combined control mode, higher efficiency can be obtained due to the minimum inlet losses, but faster dynamic response together with higher overshoot will appear. It is proved that the energy efficiency is improved, while the motion tracking performance is not degraded by introducing the multi-mode switching.

Keywords: hydraulic manipulator; energy saving; mode switching; energy regeneration; independent metering control

1. Introduction

Multi-DOF (Degree of Freedom) manipulators are always applied to various industrial and mobile machines. Electric drive systems are most commonly used to convert the input electric energy to potential and kinetic energies of the manipulator. However, the low power-density ratio restricts their applications in heavy-load mobile manipulators, such as an underwater manipulator, crane, construction machinery, agricultural machinery, etc. Characterized by high power-weight ratio, fast response, high stiffness, and high load capability, hydraulic drive systems have been widely applied in heavy-load manipulators. Other than the distributed control using the electric drive system, the control of the hydraulic drive system is centralized, of which multiple joints are supplied by one power unit. The coupling property among different joints makes the energy efficiency of hydraulic drive system lower than the electric one. Considering the environmental problems and economic benefit [1], tackling challenges related to energy efficiency and energy saving in heavy-load mobile hydraulic manipulators is a highly topical issue [2].

In a hydraulic manipulator, the hydraulic drive system converts pressure energy to potential and kinetic energies, as shown in Fig.1(a). The input mechanical energy could be provided by an electric motor or combustion engine. The pressure energy (hydraulic energy) from a hydraulic pump is distributed into multiple actuators by control valves. There

*Corresponding author. Tel.: +86 571 87952505. Fax.: +86 571 87952507.
E-mail address: benzjh@zju.edu.cn (J. Zhang).

Nomenclature			
A_a	Head side area of cylinder (m^2)	Δp_{v2}	pressure difference of meter-out valve (Pa)
A_b	Rod side area of cylinder (m^2)	q_a	Flow of head side chamber (m^3/s)
B_p	Coefficient of viscous friction	q_b	Flow of rod side chamber (m^3/s)
C_p	Leakage coefficient of pump	q_e	Difference between reference flow calculated flows (m^3/s)
E_H	Hydraulic energy (J)	q_i	Flow for each actuator ($i=1,2,3$) (Pa) (m^3/s)
E_p	Energy consumption of pump (J)	$q_{i,ref}$	Reference flow for each actuator ($i=1,2,3$) (Pa) (m^3/s)
E_s	Energy consumption of system (J)	q_s	Pump flow (m^3/s)
E_{v1}	Throttling loss of inlet (J)	$q_{s,ref}$	Reference flow for pump (m^3/s)
E_{v2}	Throttling loss of outlet (J)	q_v	Flow across valve (m^3/s)
F_L	Load force (N)	$q_{v,lim}$	Threshold of flow across valve (m^3/s)
$F_{L,lim}$	Threshold of Load force (N)	u_v	Control voltage of valve (v)
K_v	Flow-pressure coefficient of valve	u_{v1}	Control voltage of inlet valve 1 (v)
K_d	Differentiation coefficient	u_{v2}	Control voltage of outlet valve (v)
K_i	Integration coefficient	u_p	Control voltage of pump (v)
K_p	Proportion coefficient	v	Cylinder velocity (m/s)
m_L	Equivalent load mass (kg)	v_{ref}	Reference velocity of cylinder (m/s)
n_m	Rotating speed of pump (r/min)	v_1	Velocity of boom cylinder m/s)
p_a	Pressure in head side chamber (Pa)	$v_{1,ref}$	Reference velocity of boom cylinder m/s)
p_b	Pressure in rod side chamber (Pa)	v_2	Velocity of arm cylinder (m/s)
p_c	Pressure threshold of cavitation (Pa)	$v_{2,ref}$	Reference velocity of arm cylinder (m/s)
p_L	Load pressure (Pa)	v_3	Velocity of bucket cylinder m/s)
p_{Li}	Load pressure for each actuator ($i=1,2,3$) (Pa)	$v_{3,ref}$	Reference velocity of bucket cylinder (m/s)
p_{Ls}	Maximum load pressure (Pa)	V_p	Pump displacement (cc/r)
p_m	Pressure margin between pump and load (Pa)	θ_s	Pump swivel angle (deg)
p_{min}	Permitted minimum chamber pressure (Pa)	$\theta_{s,max}$	Maximum pump swivel angle (deg)
p_{ref}	Reference pressure in rod side chamber (Pa)	$\theta_{s,ref}$	Reference pump swivel angle (deg)
p_r	Drain pressure (Pa)	η_h	Overall Energy efficiency of hydraulic system
p_s	Pump supply pressure (Pa)	η_m	Mechanical efficiency of pump
Δp_v	pressure difference across valve (Pa)	η_p	Efficiency of pump
Δp_{v1}	pressure difference of meter-in valve (Pa)	η_v	Volume efficiency of pump

are mainly three types of energy losses which influence the energy efficiency: mechanical and volume losses of the pump, together with throttling losses of valves. The improvement of the pump efficiency requires the performance matching between the load and engine [3]. Generally, a constant rotating speed of the engine is utilized, thus only the throttling losses of the hydraulic drive system are aimed to optimize the energy efficiency. On one hand, the single pump provides an adequate amount of oil to the lifting actuators to drive the manipulator reaching the desired position. There are significant differences in pressure and flow among different actuators. Thus, discrepant pressure and flow lead to pressure losses across the valve orifices. On the other hand, during the lowering of the manipulator, the potential energy is often converted into heat in a speed-controlling valve without converting the energy back into recycling energy. Therefore, how to regenerate dissipative potential energy and simultaneously decrease the pressure losses across orifices are the key points to improve the energy efficiency of a hydraulic manipulator. A common approach to improve efficiency with a conventional proportional directional valve is adapting the system pressure to the highest load pressure [4]. In this system, both the pump and valve have only one operating mode, which loses the flexibility towards energy recovery and decreases of pressure losses [5]. The energy efficiency is accepted only if the current highest load is significantly lower than the maximum nominal load, yet the light load and especially gravity load still cause substantial losses.

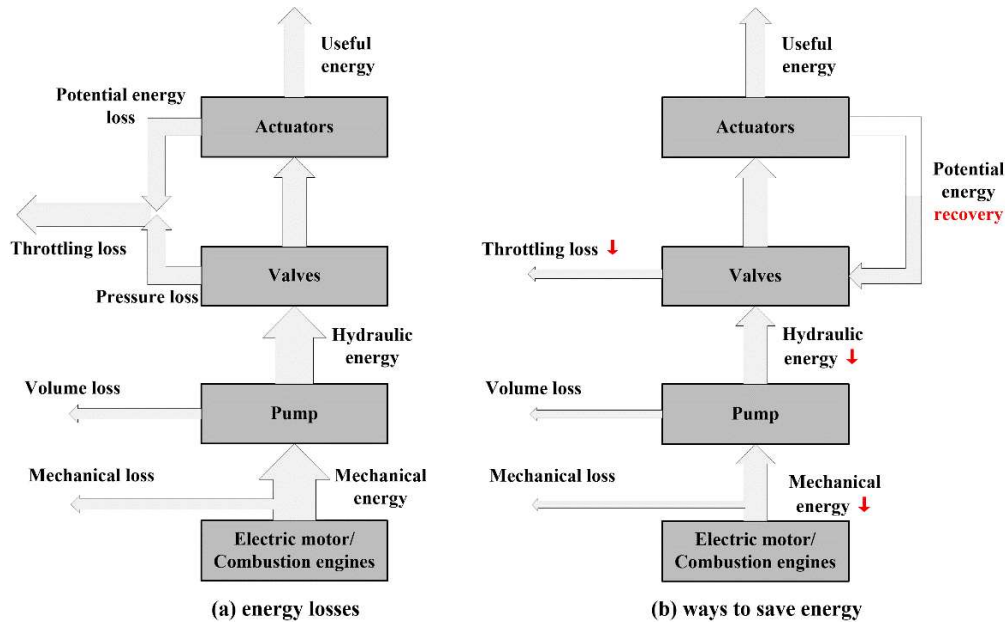


Fig.1 Energy conversion of the hydraulic drive system

Multi-mode switching is a good solution to improve energy efficiency because the operating mode could switch flexibly to adapt changeable working conditions with low energy consumptions. Multi-mode switching has been employed in various energy conversion systems. Liu et al. applied mode switching control to dual-evaporator air-conditioning systems [6]. Wen designed a hybrid-mode two-phase interleaved boost converter to improve efficiency and the power density of the fuel cell electric vehicle [7]. Wang presented hybrid control modes, including series control mode, parallel control mode, and braking control mode, to decrease the fuel consumption of a heavy-duty electric powertrain [8]. Solouk et al. developed a multi-mode engine of an electrified powertrain to improve fuel efficiency, of which operation modes include HCCI, RCCI, and SI [9]. Nazih et al. introduced a turbocharger system that operates in two different modes [10]. Therefore, the multi-mode switching is also a prominent alternative to substitute the single mode operation in the conventional hydraulic drive system.

The commonly used approach is to supplement the energy regeneration system (ERS) to construct a hybrid power system. Then the system including renewable energy, such as lowering potential energy or braking energy, can be operated as an energy regeneration mode rather than the normal mode. There are well-known types of ERSs including hydraulic type (e.g. accumulator), electric type (e.g. a battery or a combination with a supercapacitor, as well as an electric motor/generator) and mechanical type (e.g. flywheel) [11]. They have been applied to various hydraulic manipulators to save energies. For example, an ERS using an accumulator has been employed for a hydraulic crane [12]. ERSs of excavators were presented based on accumulators with a number of proportional valves [13] or switch valves [14]. Similarly, ERSs based on accumulators were applied for the excavator applications together with a three-chamber cylinder [15] or an asymmetric pump [16]. With respect to electric regeneration systems, a hybrid power excavator was

designed by integrating a supercapacitor [16]. The permanent magnet synchronous motor/generator was investigated [18] and it has been applied in the ERSs of a forklift [19] and mobile machinery [20].

With these regeneration approaches, the throttling losses of overrunning load (e.g. a gravity load) can be cancelled out, as shown in Fig.1(b). However, these recoverable forms of energy require extra mechanical, hydraulic or electric component. Therefore, they are only utilized for recovering the potential energy of the actuator with heaviest load (e.g. boom of excavator), not available for other light-load actuators. Light-load actuators still sometimes withstand overrunning loads and a spot of potential energy will be dissipated. Furthermore, additional energetic potentials from the reductions of pressure losses are not taken into account. Therefore, it is not enough to obtain an optimal energy efficiency of multi-actuator hydraulic manipulator only by the energy regeneration system.

To address the above issues, independent metering control valves were proposed to decouple the inlet and outlet such that the operating modes of valves can be extended with an electronic way. Thus, the potential energy under the overrunning load can be recovered and simultaneously part of the pressure loss under resistive load can be decreased. Eriksson summarized the feasible operating modes pertaining to different hardware layouts of independent metering control [21]. By introducing multiple modes, Lu and Yao designed energy-saving adaptive robust control of a hydraulic manipulator [22]. Choi et al. studied the energy-saving performance of excavator hydraulic systems through regeneration modes [23]. Kolks et al. proposed a smooth mode switching algorithm towards multi-mode transfers [24]. Mattila et al. studied the independent metering control of a three-DOF redundant hydraulic robotic manipulator [25]. The triple control modes of piston position, piston force, and chamber pressure tracking are designed [26]. Although the basic energy-saving principle and reactive mode switching with independent metering control valve are investigated, the effectiveness of pump control mode in efficiency improvement has rarely been addressed together, which restricts the further extensions of operating modes and accompanying efficiency improvement.

To further improve the energy efficiency, Quan et al. presented a pump flow control mode to replace the pressure control mode of load sensing pump [27], and then they introduced pressure-flow hybrid pump control modes into the independent metering system for the excavator [28]. However, the multi-mode configurations between pump and valve are not involved in, and these researches were measured by several simple actions, such that the energy-saving characteristic of independent metering control and its effectiveness in efficiency improvement are not fairly evaluated. Therefore, the efficiency improvement with multi-mode switching is still expected to enhance in the hydraulic manipulator application.

This study aims an in-depth analysis of the mode switching with independent metering control for efficiency improvement of the hydraulic manipulator. A novel electro-hydraulic drive system which enables extended control

degrees of freedom is presented by integrating independent metering valves and an electrically controlled pump. Accordingly, the possible control modes for the cylinder, valve, and pump are all constructed. A systematical configuration about the different operating modes is conducted and the corresponding multi-variable control approaches are first developed. Considering the coordinate control of pump and valve, the energy-saving characteristic for a typical duty cycle of an excavator manipulator is therefore evaluated. The energy-saving performance with the mode-switching strategies is verified by the experimental results in comparison to the conventional hydraulic drive system.

2. Problem Statement

In a hydraulic drive system, the pump is used to convert mechanical energy into hydraulic energy. Its energy efficiency is given with respect to mechanical and volumetric losses as:

$$\eta_p = \eta_m \cdot \eta_v \quad (1)$$

The volumetric loss is mainly caused by the leakage which varying with the supply pressure, displacement angle and rotating speed, so the volumetric efficiency η_v is given by:

$$\eta_v = 1 - \frac{C_p p_s}{n_m V_p} \quad (2)$$

The input energy of the pump is given as:

$$E_s = \int p_s q_s dt \quad (3)$$

Due to the constant rotating speed of the pump, the mechanical efficiency of the pump is neglected. Thus, the energy loss of the pump is derived as:

$$E_p = \frac{E_s}{\eta_v} (1 - \eta_v) \quad (4)$$

The velocity of each actuator is regulated by the control valve. Thus, inlet and outlet pressure losses are calculated as:

$$E_{v1} = \Delta p_{v1} \cdot q_a \quad (5)$$

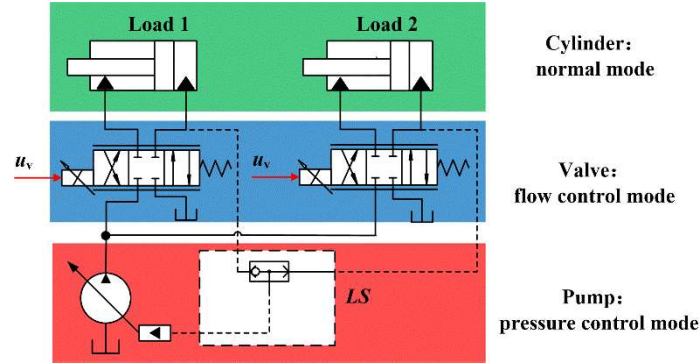
$$E_{v2} = \Delta p_{v2} \cdot q_b \quad (6)$$

The energy efficiency of the hydraulic system is given by:

$$\eta_h = 1 - \frac{E_{v1} + E_{v2} + E_p}{E_s + E_p} \quad (7)$$

Conventional electro-hydraulic control systems, for example, load sensing (LS) systems, are commonly used hydraulic drive systems that make trade-offs between energy efficiency and steering quality, as shown in Fig.2. Firstly, the pump is regulated in the pressure control mode with a hydro-mechanical way, where the pump is pre-set to maintain a certain pressure margin over the load-leading meter-in valves. Therefore, the inlet pressure losses are held constantly by the supply pressure control. Second, a proportional directional valve features meter-in and meter-out edges with mechanical coupling through the valve spool. There is only one control signal, the spool position, to regulate the

133 actuator flow regardless of different load characteristics. Therefore, the control mode of the valve is also sole.
 134 Furthermore, due to the mechanical coupling between the inlet and outlet in the directional control valve, the flow is
 135 only charged into one cylinder chamber from the pump and then discharged to the tank from another cylinder chamber,
 136 which is referred as normal mode. As shown in Table.1, four columns represent different operating conditions with
 137 respect to the directions of the motion and load force. All the conditions are operated under normal modes.



138 **Fig.2** Conventional load-sensing system and its control mode

139 **Table.1** Single operating mode of the cylinder in the conventional system

140

Load condition				
Normal mode (NO)				

141
 142 The simple control modes for the hydraulic drive system will lead to the following energy loss, as shown in Fig.3:

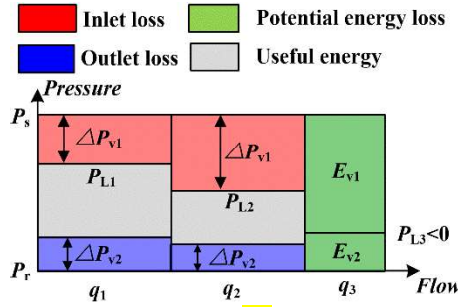
143 **Inlet losses:** It is mainly caused by the single mode of the pump. The pressure margin p_m is set to overcome losses
 144 across the hoses, directional control valves and pressure compensation valves. To satisfy the requirements of all
 145 operating points, the pump always considers the worst working conditions to preset the pressure margin, which causes
 146 unnecessary inlet pressure losses Δp_{v1} . Besides, for a multi-actuator system, the system pressure is determined by the
 147 heaviest load, such that there exists large Δp_{v1} in the light-load actuator due to the load difference.

148 **Outlet losses:** It is caused by the single mode of the valve. Due to the mechanical coupling of the inlet and outlet, the
 149 meter-out valve cannot be operated in the pressure control mode separately. Therefore, the outlet orifice cannot open as
 150 large as possible under resisting loads, leading to a noticeable outlet pressure loss Δp_{v2} .

151 **Potential energy losses:** It is mainly caused by the single mode of the cylinder. Under overrunning loads, the supply
 152 flow is still required from the pump to lower loads such that the inlet energy losses E_{v1} is inevitable. Besides, the

153 potential energy cannot be recuperated and is wasted as outlet energy losses E_{v2} .

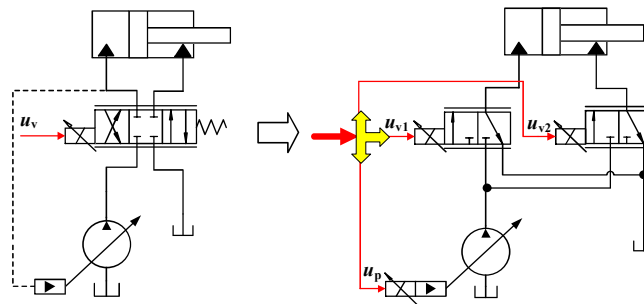
154 Due to the three aspects, the problem of low energy efficiency is serious in the conventional hydraulic system.



155
156 Fig.3 Energy losses of the conventional system

157 3. Electronically tunable operating modes

158 To improve the energy efficiency of a hydraulic manipulator, the category of operating modes should be extended
159 such that it can be tuned online to adapt to different load characteristics. This study designs a novel electronic-hydraulic
160 drive system with multiple control DOFs, as shown in Fig.4. In contrast to conventional directional valves, the
161 independent metering control valve is utilized which allows the individual control of meter-in and meter-out edges. The
162 first benefit of such decoupling controlled orifices allows individual fluid flow paths such that regeneration modes on
163 the low or high-pressure side are allowed. Therefore, the single normal mode of the cylinder from the high-pressure
164 supply to the expanding displacement volume, and from the contracting displacement volume to the low -pressure
165 return line can be suspended, as shown in Table.2. In HPR modes, a small load is transformed with a smaller flow and
166 heavy load pressure such that the inlet losses Δp_{v1} owing to load difference could be diminished. In LPR modes, the
167 gravity load has a self-generated pressure that can be pumped to cause flow such that the potential energy losses could
168 be diminished.



169
170 Fig.4 Presented electronic-hydraulic drive system based on independent metering control

171 Table.2 Multiple operating modes of the cylinder

Load condition				
----------------	--	--	--	--

Normal mode (NO)				
High pressure Regeneration (HPR)				
Low Pressure Regeneration (LPR)				

172

173

174

175

176

177

178

179

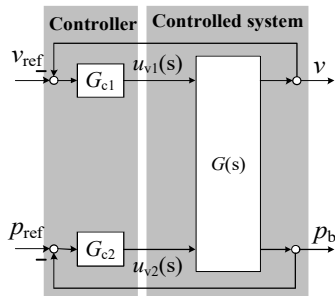
180

181

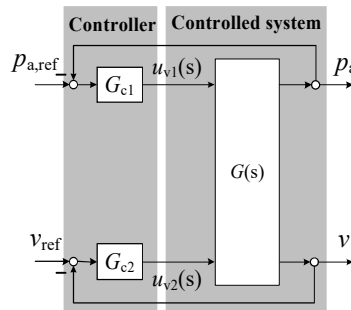
182

183

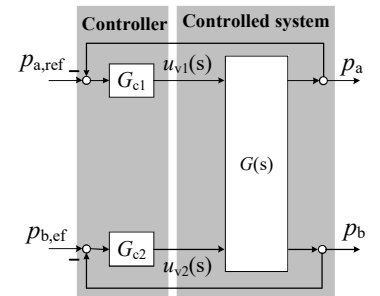
The second benefit of such decoupling controlled orifices is to offer a greater degree of freedom in terms of command variables and then multiple target-variables can be controlled. Then, both flow and pressure control modes can be achieved independently for an actuator. According to the controlled target-variables, two categories of valve control modes are feasible containing meter-in (MI) control and meter-out (MO) control. With the meter-in control mode, two individual control loops are designed to regulate the meter-in and meter-out areas, as shown in **Fig.5 (a)**. The former one aims to track the required motion trajectory, while the latter one results in outlet losses to be as low as possible such that the necessary supply pressure can be decreased. Due to the individual control loops of motion and pressure, functions of the two orifices can be exchanged, which is referred to as meter-out control in **Fig.5 (b) and (c)**. The meter-out control concept is defined as that the throttling losses are shifted from the meter-in to meter-out side. Thus, inlet pressure losses can be decreased due to its large opening to optimize energy efficiency. The pressure or the velocity of the actuator are controlled by the meter-out valve.



(a) Meter-in control mode



(b) Meter-out flow control mode



(c) Meter-out pressure control mode

Fig.5 Multiple valve control modes

184

185

On the basis of decoupling controlled orifices, additional energy-saving potentials, which exist for inlet pressure losses with load sensing structures, are the further subject of this study by using an electrically controlled pump in **Fig.6**.

Force limitation of potential energy regeneration

When lowering a gravity load, both cylinder chambers are connected to the tank under LPR mode, and the load has a self-generated pressure that can be pumped to cause flow. As the manipulator moves down, the gravity load may decrease until it cannot overcome the friction, inertia force, and back pressures. Fig.7 exhibits the movement of a cylinder driven by its gravity load. All measurements pertaining to different velocities demonstrate that the cylinder will tend to stop when the gravity load decreases to a threshold. The threshold represents a force limitation when LPR modes must be switched out. It is calculated according to the force balance equation as Eq. (8) or (9).

$$m_L \dot{v} = F_{L,lim} + p_a A_a - p_b A_b - B_p v \quad (8)$$

$$m_L \dot{v} = F_{L,lim} + p_b A_b - p_a A_a - B_p v \quad (9)$$

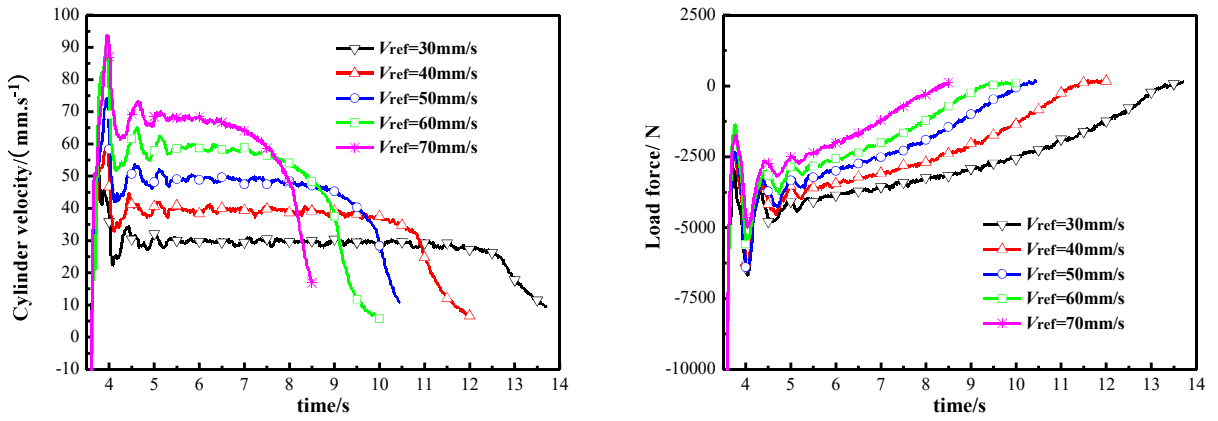


Fig.7 Experimental results of potential energy regeneration for excavator arm extension

Flow Limitation of potential energy regeneration

To recuperate the potential energy, the supply flow is switched from pump to suction from the tank under LPR mode. However, the flow from the tank should also cross pipelines and valve orifices with a certain pressure loss. If the pressure loss exceeds the low-level drain-line pressure, the inlet chamber would encounter with cavitation. Hence, the LPR mode can be enabled and disabled according to how much flow is available in the drain line. The information on how much flow pertaining to the valve throttling characteristics can be approximately estimated as:

$$q_{v,lim} = K_v \sqrt{p_r - p_c} \quad (10)$$

To avoid cavitation under LPR modes, the drain-line pressure should be enhanced to expand the operating range of the potential energy regeneration. A simple way of doing so is to have an electrically controlled relief valve or check valve in the return line. In this study, a check valve with 0.2 MPa cracking pressure is mounted before the tank such that the operating ranges of LPR modes can be enlarged, as shown in Fig.8.

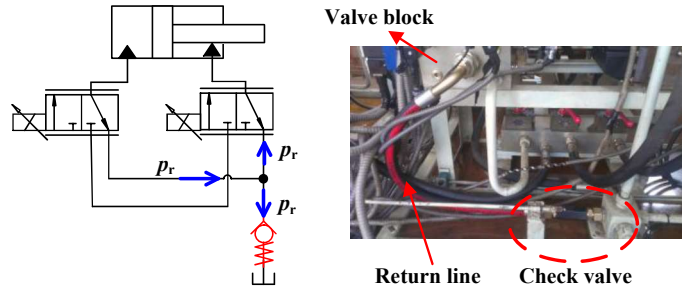


Fig.8 Enhanced tank pressure by a check valve

Taking the operation limits into account, the cylinder mode is selected according to the load quadrants, which are defined by the four combinations of the axial directions of load force and actuator velocity (shown in Fig.9). In view of the energy efficiency, the LPR mode has higher priority than the normal one when there exist overrunning loads (Qua.II and Qua.IV) unless the cylinder encounters with force or flow limitations. If so, the LPR mode has to switch to the normal one to track the required motion. Under the resistive load, the normal mode has a higher priority for the heavy load. If there exists a light resistive load, HPR mode is recommended to reduce the supply flow.

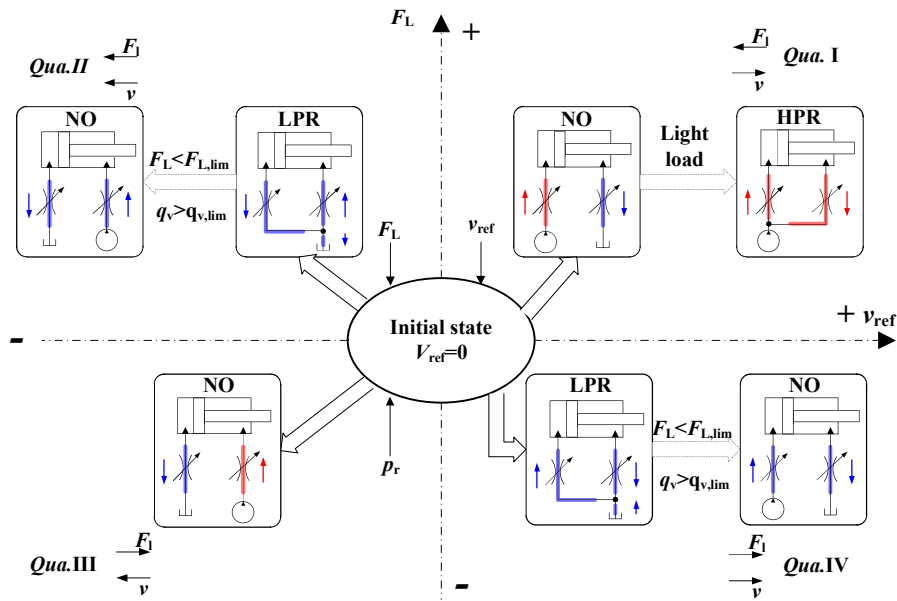


Fig.9 Cylinder mode selection for the four-quadrants load

4.2 Modes Configurations among cylinder, valve, and pump

To take advantages of energy regenerations to improve the efficiency, the operating modes of the cylinder are dominant compared with modes of valve and pump. It means that the configurations of valve and pump modes should comply with the selections of cylinder modes.

Under the overrunning loads, the actuator may be out of control to fall down rapidly, and the supply flow from pump or tank would be possible to encounter with cavitation when the valve utilizes MI control mode. Therefore, the MO valve control mode must be selected in these cases. If all the operating conditions are not beyond the mode capability, then regeneration modes are selected in the cylinder and the pump runs with the idling state (PI mode). Otherwise, the

250 cylinder still works under the NO mode, and PP control mode is a better selection for **the pump** because the cylinder
 251 pressure can be directly controlled by the pressure feedback to avoid cavitation. The mode configuration for
 252 overrunning loads is depicted in **Figs.10(a) and (b)**.

253 Under the resistive loads, both the two optional categories of valve control modes can be employed. There are two
 254 feasible combinations of valve and pump modes, as depicted by the red and blue lines in **Fig.10(c)**. The first one utilizes
 255 meter-in valve control together with pump pressure control (PP_MI), and the other one utilizes meter-out valve control
 256 together with pump flow control (PF_MO). Meter-in valve control is not suited to pump flow control due to the
 257 potential problem of overmatching between the supply flow and valve orifice flow.

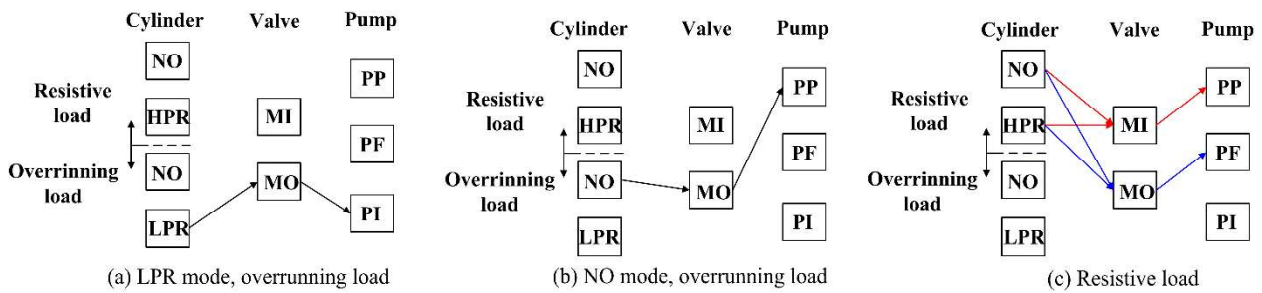


Fig.10 Mode configuration among cylinder, valve, and pump

258 In the framework of multi-mode configurations, the energy-saving capability pertaining to different load
 259 characteristics **is enhanced** compared with the conventional hydraulic drive system. However, both two objectives of
 260 optimal energy efficiency and precise motion control should be further carried out by the multi-variable controller.

261 **5. Multi-variable control design**

262 Due to the distinguishing feature between the resistive load and overrunning load, the multi-variable controllers are
 263 designed separately for the following two conditions.

264 **5.1 Multi-variable controller under resistive loads**

265 The difference between the PP_MI and PF_MO modes can be captured by the multi-variable control approaches, as
 266 shown in **Fig.11**. PP_MI mode employs a three-input and three-output (TITO) controller. The supply pressure **is**
 267 **regulated beyond** the load pressure by the preset pressure margin p_m . MI valve controllers are designed as: the meter-in
 268 valve controls the input actuator velocity to distribute the supply flow, and meter-out valve controls the reference
 269 backpressure to reduce the outlet pressure loss and simultaneously avoid the cavitation. In contrast, PF_MO mode
 270 employs a dual-input and triple-output controller (DITO) without the pressure margin input. The pressure feedback is
 271 cancelled out and the supply flow is regulated according to the input velocities of all actuators. The meter-in valve is
 272 endeavored to decrease the inlet pressure losses and the flow or pressure of each actuator is controlled by the meter-out
 273 valve. Next, the detailed multi-variable controllers for PP_MI and PF_MO modes are designed in **Fig.12**.

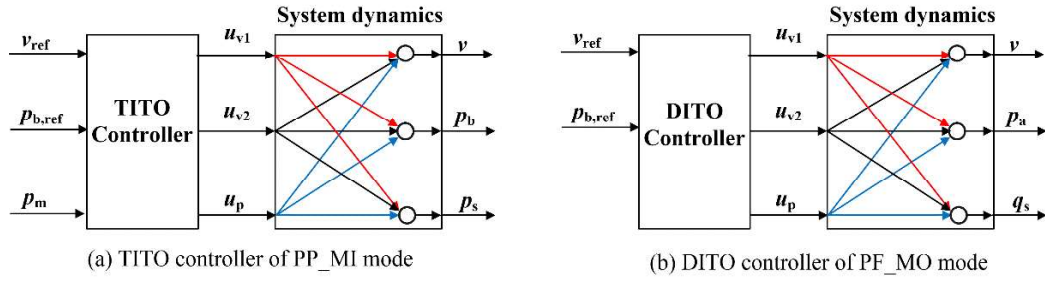


Fig.11 Multi-variable control block diagrams

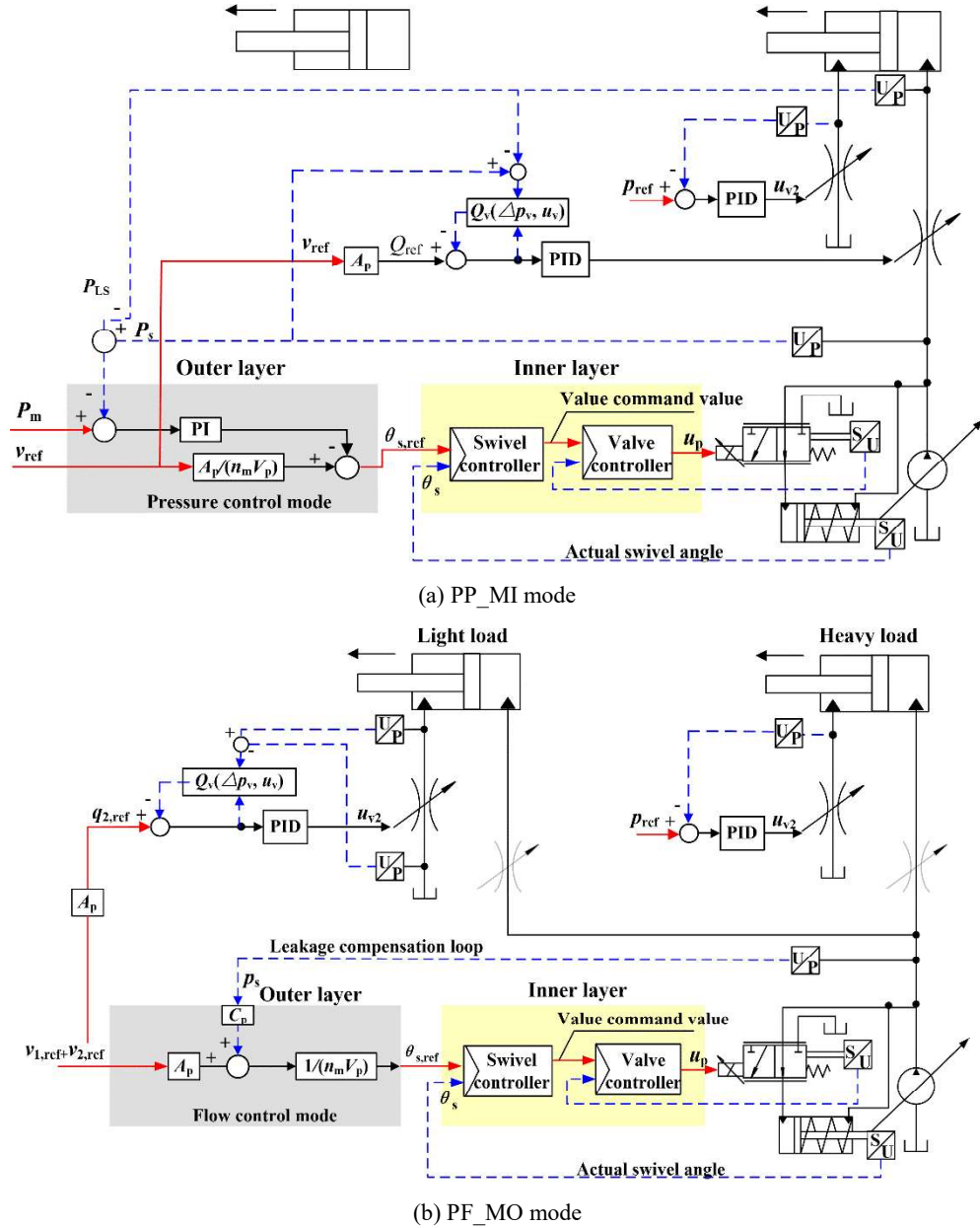


Fig.12 Multi-variable control under resistive loads

274 The pump controller contains two layers. An inner layer controller consisting of valve and swivel controllers are used
 275 to regulate the pump displacement with the feedbacks of swivel angle and valve position. The reference swivel angle to
 276 the inner layer controller is calculated by an outer layer. PP and PF control modes of the pump are implemented in the
 277 outer layer. PP controller includes a PI regulator to track the reference pressure margin. However, the pump dynamic

depends on the PI parameters, which will encounter poor response and instability. To decrease dependence of PI parameters and improve the pump dynamic, a feedforward block to calculate the theoretical swivel angle is added such that only a smaller output of PI regulator around the reference signal of swivel angle is required. PF controller only uses the feedforward block as the primary method to determine the swivel angle and eliminate the pressure feedback loop. This feedforward block utilizes a mapping from pump flow to swivel angle by applying Eq. (11), of which supply pressure and rotate speed are included. This arrangement can compensate for the leakage flow with respect to the swivel angle and pump pressure.

$$u_p = \frac{\theta_{s,ref}}{\theta_{s,max}} = \frac{\sum q_{i,ref} + C_p p_s}{n_m V_p} \quad (11)$$

The valve controller contains two loops: velocity and pressure control loops, which are both designed based on the pressure feedbacks. A calculated flow feedback controller is employed to implement velocity tracking. Taking PP_MI mode for instance [Fig.12(a)], the control signal of the meter-in valve is given by a PID regulator based on the difference q_e between the reference flow q_{ref} and the actual one q_v .

Generally, the actual flow q_v is calculated utilizing a non-linear flow mode of the valve orifice in Eq. (12). The flow model has been calibrated off-line as a hydraulic conductivity coefficient K_v :

$$Q_v = K_v(u_v, \Delta p_v) \sqrt{\Delta p_v} \quad (12)$$

where the hydraulic conductivity coefficient K_v is subject to spool displacement, temperature and pressure difference. The calculated flow feedback controller eliminates the non-linear dependency of load pressure such that the cylinder is able to precisely track the reference velocity under uncertain and time-varying loads.

In terms of the pressure difference $p_{b,e}$ between reference one p_{ref} and actual one p_b , the closed loop pressure control is also implemented by means of PID regulator to reduce the outlet pressure loss. Here p_{ref} refers to the minimum pressure resisting cavitation.

It is noted that under PF_MO mode, the meter-in valves for all the actuators are opened fully to obtain the lowest inlet pressure losses. How to achieve precise motions for different actuators is another question when there are only meter-out valves under control. As shown in Fig.12(b), the heavy load in the system uses meter-out pressure control to reduce the supply pressure, and light loads and other loads under non-normal modes (LPR or HPR modes) are operated by meter-out flow control to distribute the supply flow. The flow of the heavy load is determined by the subtraction between regulated supply flow and light load flows. This measure also eliminates the over-matching problem with the pump PF mode because excessive supply flow can be accepted by the heavy load.

5.2 Multi-variable controller under overrunning loads

The detailed multi-variable controller under overrunning loads are described in Fig.13. Under the regeneration mode,

the motion of the actuator is tracked by the meter-out valve. The meter-in valve is also forced to open fully. The measure has two positive effects. The inlet pressure losses are decreased as much as possible, and the ability to resist cavitation is also enhanced. If the operating condition is beyond the mode capability, the normal mode is switched on, and the cylinder pressure is endeavored to track the reference value 0.3 MPa with a pump pressure controller such that a chamber pressure beyond the threshold of cavitation is guaranteed.

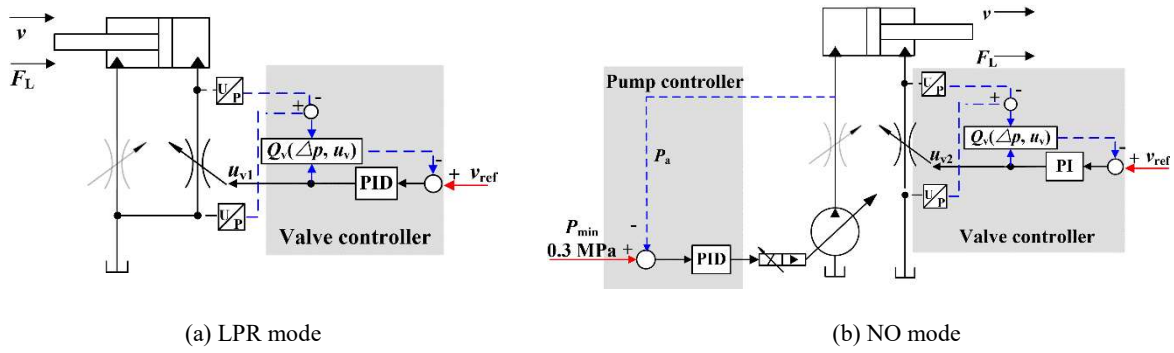


Fig.13 Multi-variable control under overrunning load

6. Energy-saving analysis

According to the designed mode switching and multi-variable control systems, energy consumptions using different mode switching approaches are analyzed in a three-actuator condition. The assumption is made that all the operating conditions are not beyond the mode capability. As shown in Fig.14, Load 1 is defined as the heavy resistive one, Load 2 is defined as the light resistive one and Load 3 is defined as a lowered gravity one. According to the logic control in Fig.9, the cylinder modes of the three loads are NO, HPR and LPR respectively.

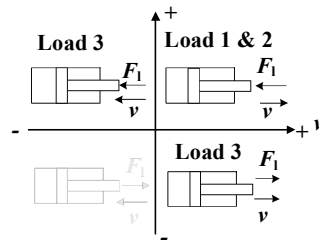


Fig.14 The distributions of three loads

For Load 1 located in *Qua.I*, the outlet pressure losses of both PP_MI and PF_MO mode are decreased compared with the conventional system due to the decoupling of inlet and outlet. The inlet pressure losses with PP_MI mode can also be reduced by diminishing the pressure margin. Compared with PP_MI, inlet pressure losses with PF_MO is given by the resistance in the hoses and fully opened the meter-in valve, which can be further decreased to a minimum level. Therefore, the system pressures of both PP_MI and PF_MO mode are decreased in terms of pressure losses.

Although located in *Qua.I*, Load 2 is changed to HPR mode both with PP_MI and PF_MO modes because it is the lower load compared with Load 1. Therefore, both the head and rod sides are charged and discharged by pressure oils.

With a decrease of supply flow into Load 2, the energy consumptions are reduced compared with the conventional system. Apart from the decreased flow, due to the decrease of supply pressure, another energy-saving way comes from the diminution of inlet losses caused by the difference between Load 1 and Load 2.

Owing to the location in *Qua.II* or *Qua.IV*, Load 3 is changed to LPR mode. It is driven by making use of the lowering load without any supply flow from the pump, so the energy consumptions of Load 3 are completely omitted compared with the conventional system. In this case, there are no further improvements in energy efficiency using PF_MO compared with PP_MI.

In a summary, the energy-saving performance in contrast to the conventional system is exhibited in Fig.15. Both PP_MI and PF_MO modes have prominent advantages on decreases of the outlet and potential energy losses by the flexible transfer of operating modes. Additionally, PF_MO mode has higher efficiency than PP_MI mode because of further improvements of inlet pressure losses.

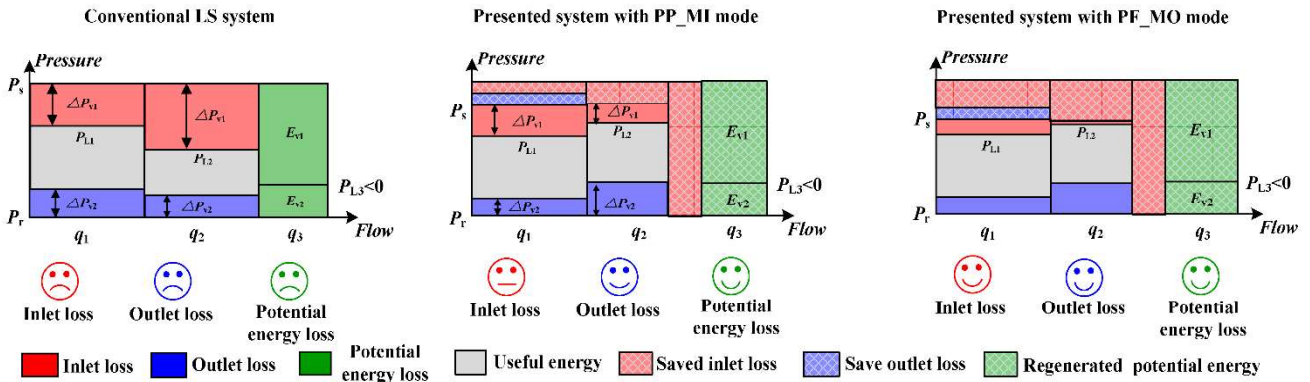


Fig.15 Energy efficiency analysis of multi-mode switching

7. Measurement System

To have a good knowledge of working performance and energy efficiency with the tunable operating modes, a heavy-load hydraulic manipulator of 2-ton excavator with three DOFs is studied as an example in this paper. Its hydraulic drive system consists of proportional directional valves (PDV) and an electrically controlled pump, in which a general system structure featuring a maximum control DOF is constructed, as shown in Fig.16. Two PDVs feature two variable orifices per cylinder displacement volume: one high-pressure valve and one low-pressure valve each. Additionally, multiple control modes of the pump are considered by means of the electrically controlled pump. Feasible pressure and flow control modes can be differentiated by the availability of control software. To determine the operating modes by control software, pressure sensors of four ports for an actuator are mounted. Velocity/displacement sensors, as well as a supply flow meter, are also included to measure the system states but not used in the controller. The digital control system is developed under the XPC Target Real-time Workshop containing a host and a target computer. The real-time signal acquisition and control applications are both carried out on the MATLAB/Simulink software platform.

353 Main parameters of the measurement systems are listed in the following Table.3.

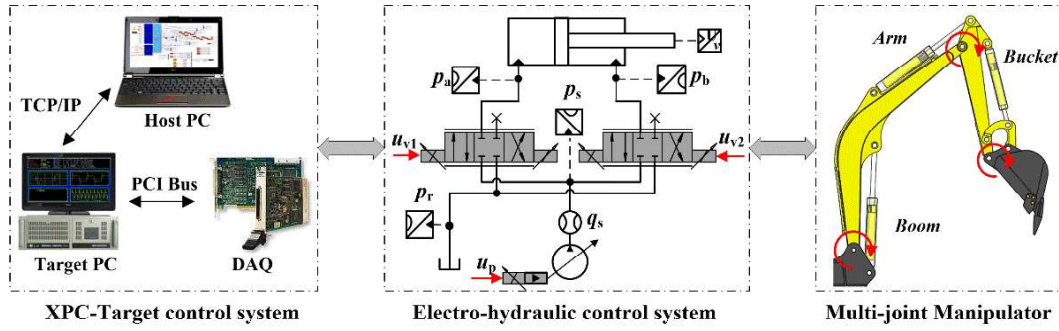


Fig.16 Structure of measurement system

Table.3 Descriptions of the experimental setup

Component	Specifications
Proportional directional valve	Rexroth 4WREE10E50
Electronic controlled pump	Rexroth SYDFEE-2X/045R-PPA
Boom cylinder	0.07 m (head diameter)/0.04 m (rod diameter)/ 0.411 m (stroke)
Arm cylinder	0.07 m (head diameter)/0.04 m (rod diameter)/ 0.4 m (stroke)
Bucket cylinder	0.06 m (head diameter)/0.035 m (rod diameter)/ 0.375 m (stroke)
Electric motor	ABB QABP180L,22kw B35 380V/50HZ 4P
Data Acquisition (DAQ) Card1	NI PCI-6229
Data Acquisition (DAQ) Card2	NI PCI-6713
Pressure sensor	CYB100-20 (4-20mA, 0-20MPa, 24VDC supply)
Velocity sensor	MTS RP S 0440M D60 1 A41
Flow sensor	VSE-VS1 (Flow range: 0.05-80 L/min)

357 For this experimental measurement, the uncertainty analysis should be evaluated to capture the error range of a
 358 measured parameter [30]. The Schultz and Cole method for uncertainty analysis was utilized. Assuming that an indirect
 359 measurement combines a series of direct measurements, the compound uncertainty ΔR is given as [31]:

$$360 \quad \Delta R = \left[\sum_{i=1}^n \left(\frac{\partial R}{\partial x_i} \Delta x_i \right)^2 \right]^{1/2} \quad (13)$$

361 where ΔR is the compound uncertainty, Δx_i ($i=1,2,3,\dots, n$) is the error of each direct measurement.

362 Uncertainties of the measurement components are listed in Table 4. In this paper, cylinder velocities, pressures and
 363 flows are measured directly by the XPC-Target control system. The hydraulic power or energy are calculated by the
 364 multiplication of the supply flow and pressure, as exhibited in Eq. (3). Therefore, the relative uncertainties of these
 365 parameters are calculated in Table.5.

366 Table.4 Uncertainties of the measurement components

Components	Measurement accuracy
Pressure sensor	0.25%
Velocity sensor	0.5%
Flow sensor	0.3%
Analog input of DAQ Card	0.016%
Signal procession module between DAQ cards and sensors	0.1%

Table.5 Relative uncertainties of experimental parameters

Parameters	Relative uncertainty
Pressure	0.270%
Velocity	0.51%
Flow	0.317%
Hydraulic Power	0.416%

8. Case Study

To analyze the energy-saving potentials that emerge through flexible operating modes, a duty cycle that puts as many technical challenges as possible should be selected. In this paper, a continuous duty cycle involving all the three actuators is measured in Fig.17. The set trajectory of each actuator is depicted in Fig.18. The cycle lasts for about 15 seconds and includes a series actions simulating the manipulator lifting the three actuators, lowering the boom, retracting the bucket to scoop up material, moving out from the pile, forwarding to a dump truck and unloading the material from an unloading position.

Three different systems are evaluated by this duty cycle. The present hydraulic drive system with PP_MI and PF_MO modes are both measured compared with the convention load sensing (CLS) system. The pump displacement in the CLS system is regulated with a pressure control way to simulate the conventional hydro-mechanical load sensing mechanism. The pressure margin between supply and load pressures is set to a constant value of 1.2 MPa in the CLS system.

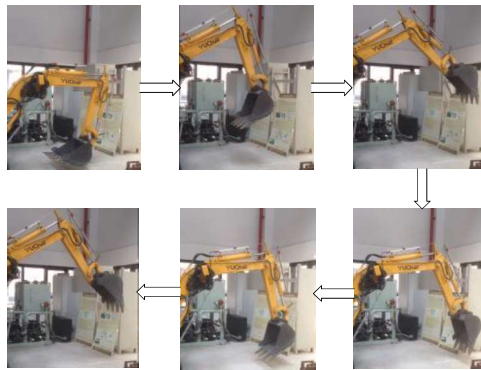


Fig.17 Studied duty cycle of the measurement machine

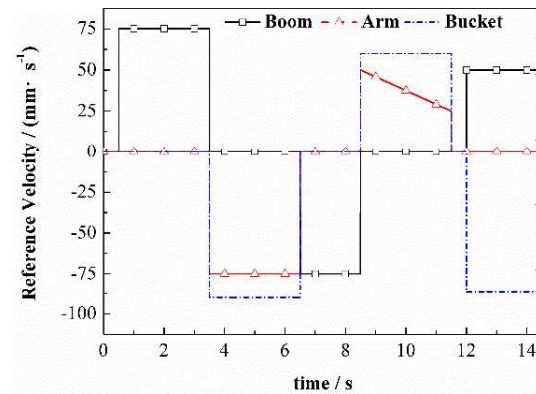


Fig.18 Reference velocity of three actuators

The cylinder modes for different actuators are marked with different fill patterns, as shown in Fig.19. During the time range of 8.5s to 11.5s, both the arm and bucket retract under overrunning loads. However, only the load of the bucket has insufficient capability to drive the movements. Therefore, the mode of arm switches to LPR one, but the mode of bucket still switches to the normal one. When the boom is lowering down, the normal modes in the CLS system is obviously switched to LPR modes in the present system due to the large gravity load. The velocity tracking errors are depicted in Fig.20.

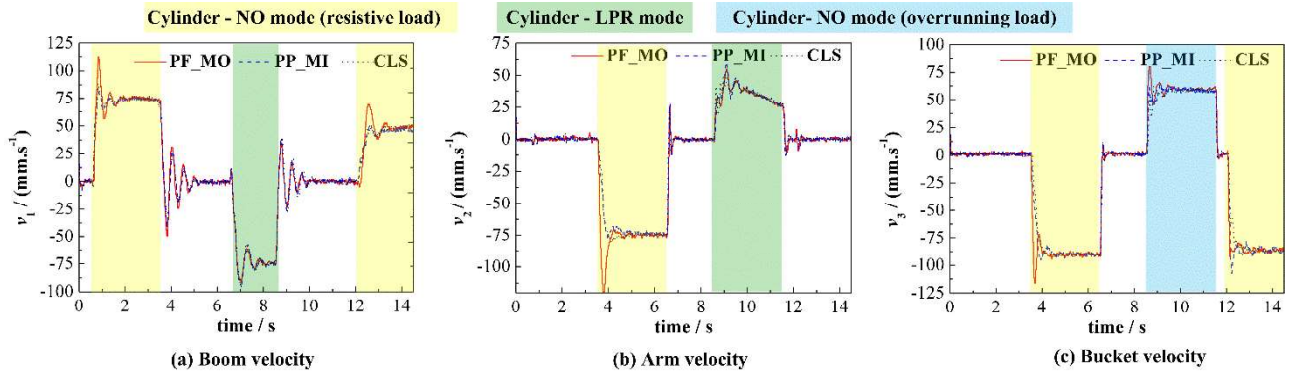


Fig.19 Comparison of motion tracking performance

Very good motion tracking can be obtained for all three hydraulic drive systems referring to **Figs.19 and 20**. The velocity dynamics of PP_MI is almost the same with CLS. Compare with PP_MI and CLS system, faster velocity response together with higher overshoot can be observed in PF_MO under NO modes. Such higher overshoot is caused by the abrupt maximum opening of the meter-in valve rather than a low stability margin. Actually, the stability of PF_MO is better than the other two hydraulic drive systems because of the open-loop controller. It can be confirmed that both the velocity and pressure of PF_MO rapidly decay to a steady value. Static errors of velocity trackings are consistent. In a summary, the motion tracking performance is not degraded by introducing the multi-mode switching.

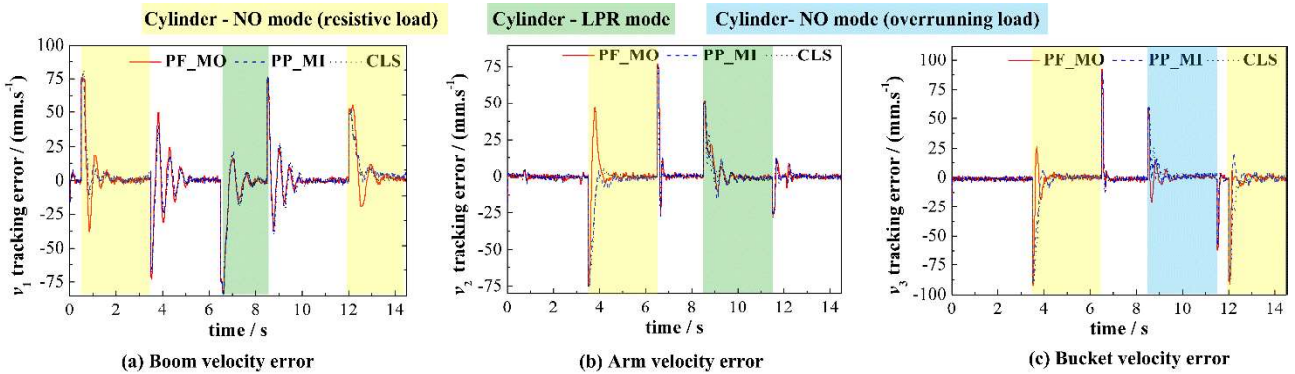


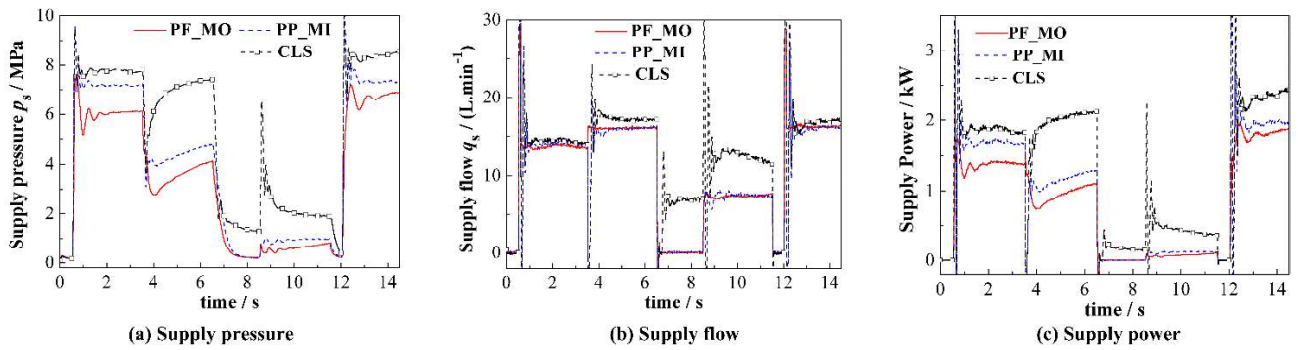
Fig.20 Comparison of velocity tracking errors

In **Fig.21(a)**, the supply pressures of PF_MO, PP_MI and CLS systems are trending down in turn for an arbitrary time. Under NO modes, the decreases in supply pressure, on one hand, arise from the decreases of outlet pressure losses. It can be captured in **Figs. 22 and 23** that the backpressures of the boom (0.5s~3.5s and 12s~14.8s), arm (3.5s~6.5s) and bucket (8.5s~11.5s) are only 0.3 MPa, which is approximatively 0.9 MPa in the CLS system (**Fig.24**). On the other hand, the optimal pressure margins using the electrically controlled pump also contribute to the reductions of supply pressures. The pressure margins of PP_MI is decreased to 0.6 ~1.0 MPa according to the flow variations. The supply pressure of PF_MO is further decreased compared with PP_MI because the pressure margins achieve only 0.25 MPa by the combination of pump flow control and meter-out valve control. With respect to potential energy regeneration periods (6.5s~11.5s), the supply pressures are of course decreased because supply flows are not required from the

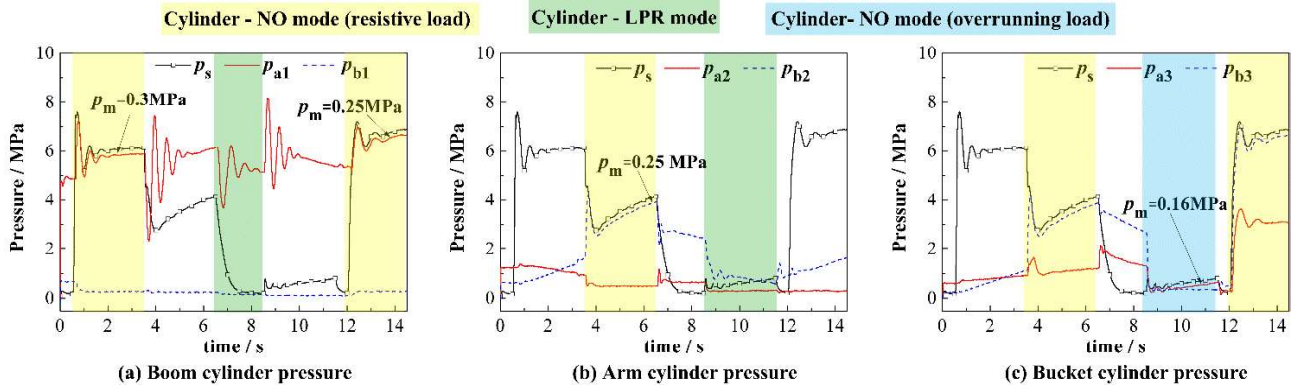
406 pump.

407 In Fig.21(b), the supply flows of PF_MO, PP_MI and CLS systems are also trending down for an arbitrary time. The
 408 tendency is obvious when potential energies are recuperated because the supply flows of PF_MO and PP_MI come
 409 from the tank rather than the pump. Under NO modes, there is no flow regeneration from the tank. In spite of this, slight
 410 decreases of supply flow still exist because less pump volume losses are obtained by lower supply pressures.

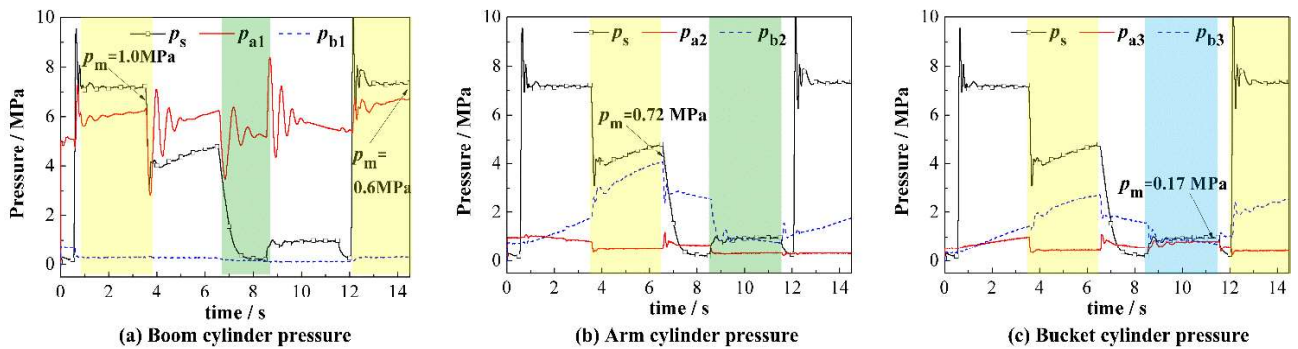
411 Following the downward trends of supply pressures and flows, the supply powers are depicted in Fig. 21(c). To
 412 analyze the energy efficiency in detail, the saved energy is also divided into three parts: decreased inlet losses,
 413 decreased outlet losses, and regenerated potential energy.



414 Fig.21 Comparison of supply pressure, flow, and power



416 Fig.22 Cylinder pressure of PF_MO mode



418 Fig.23 Cylinder pressure of PP_MI mode

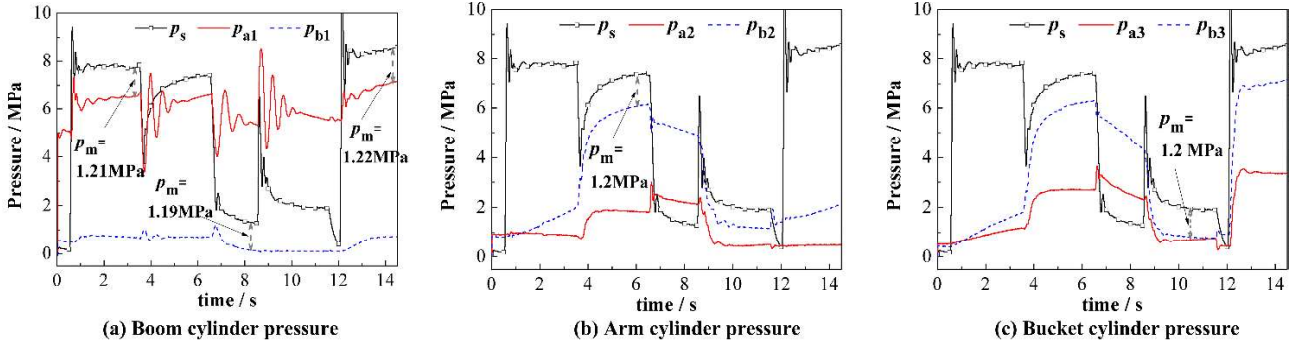


Fig.24 Cylinder pressure of CLS system

The energy consumptions for each action are given in **Fig.25(a)**. In terms of Eqs. (1) to (6), the total energy consumptions of each hydraulic drive system for the duty cycle, as well as the saved energies of the three aspects, are depicted in **Fig.25(b)**. Compared with the CLS system, the energy saving rates of PP_MI and PF_MO can reach **25.8 %** and **35.3%** respectively. Prominent energy improvements using the multi-mode switching are obtained. The primary contributions of energy saving are the decreases in pressure losses, which accounts for 81.1% and 86.2% of the total saved energy, respectively for PP_MI and PF_MO modes. The decreased outlet losses with PP_MI mode achieve 4380 J, which are obviously larger than decreased inlet losses. In contrast, the decreased outlet losses with PF_MO mode are lower than PP_MI mode, but more inlet losses (3301 J) are saved, which contributes to higher efficiency. It can be explained that the energy losses with PF_MO mode are switched from inlet to outlet. The results agree well with the theoretical analysis in **Fig.15**.

It is noted that the decreased inlet losses of PP_MI are negative, which means that its inlet losses are even larger than CLS. It can be further analyzed by the energy-saving characteristics of three actuators in **Fig.26**. In **Figs.26 (a) and (b)**, the outlet losses of both PP_MI and PF_MO modes are equal because the boom and arm are both the heavy loads during their movements and thereby their meter-out valves are both operated under pressure control modes. In **Fig.26 (c)**, during the periods including (3.5 s~6.5 s) and (12 s~14.8 s), the bucket is the light load under NO mode. Its meter-in valve with PP_MI mode is operated under flow control mode. Thus, the load difference between arm and bucket is dissipated in the inlet orifice of the bucket. Therefore, the decreased inlet losses with PP_MI mode are negative. Compared with PP_MI mode, the meter-in valve of the bucket with PF_MO mode is fully open and its meter-out valve is operated under flow control mode. Hence, obvious decreases of inlet losses can be captured with PF_MO, and decreased outlet losses with PF_MO are less than PP_MI mode. To sum up, the comprehensive reductions of pressure losses with PF_MO are larger than that with PP_MI for all the three actuators.

However, the saved energy by the potential energy regeneration is only in the minority of the total saved energy. It can be explained that the measuring machine is a mini-excavator, thereby the potential energy is relatively low. For a heavier machine such as 20 t excavator or crane, the saved energy by the potential energy regeneration using the

presented multi-mode switching method will be more remarkable.

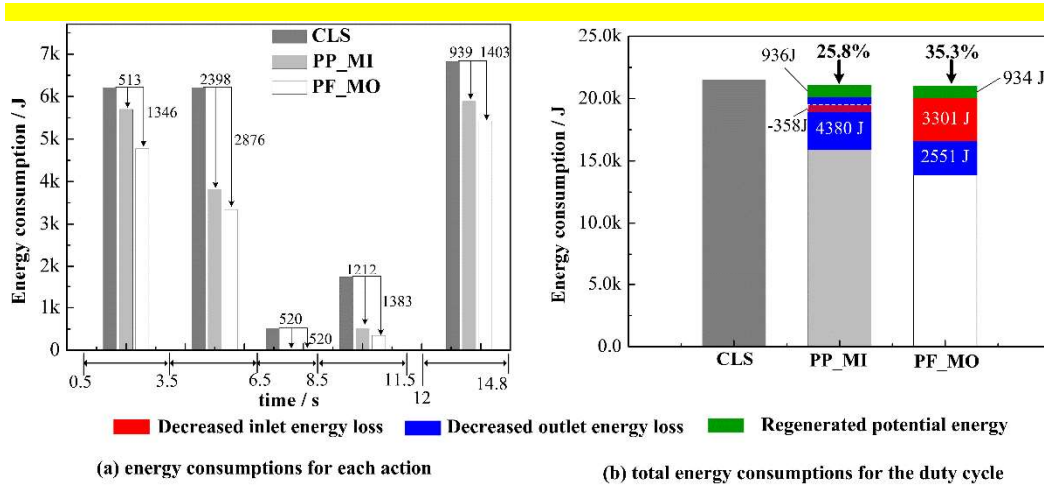


Fig.25 Experimental results of energy consumptions

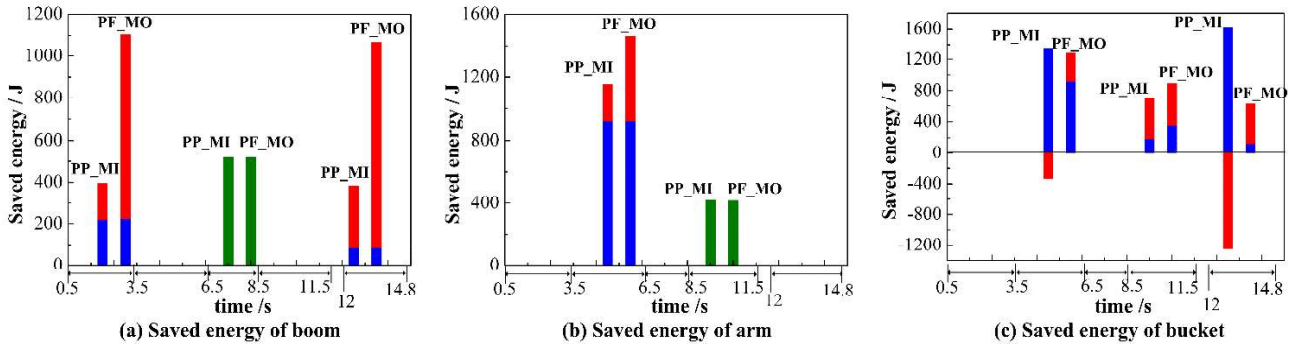


Fig.26 Saving energy of three actuators

9. Conclusions

This paper proposed a new methodology for multi-mode transfer of hydraulic drive system that assesses the technological minimum of energy demand for the heavy-load mobile manipulator. The multiple modes of the cylinder, valve, and pump are all considered using a novel designed electro-hydraulic drive system, which includes the independent metering control valves with an electrically controlled pump. Consequently, the inlet loss, outlet loss, and potential energy loss can be optimized simultaneously. Different mode configurations and their multi-variable control approaches are designed to achieve two objectives including higher energy efficiency and precise motion control. The experimental results from a duty cycle of 2 t excavator show that PP_MI and PF_MO control modes using the proposed system yield 25.8% and 35.3% energy-saving ratios, respectively. Higher efficiency using PF_MO mode can be obtained due to the minimum inlet losses. Moreover, the motion tracking performance is not degraded by using multi-mode switching.

Acknowledgment

This work was supported by the National Natural Science Foundation of China Grant (Grant No.51705152 and

464 No.91748210), NSFC-Zhejiang Joint Fund for the Integration of Industrialization and Informatization (Grant
465 No.U1509204), Chongqing Research Program of Basic Research and Frontier Technology (Grant No.
466 cstc2016jcyjA0253)

467 **Reference:**

- 468 [1] Vukovic M, Leifeld R, Murrenhoff H. Reducing Fuel Consumption in Hydraulic Excavators — A
469 Comprehensive Analysis. *Energies*. 2017, 10: 687. <http://dx.doi.org/10.3390/en10050687>.
- 470 [2] Wang H, Wang Q F, Hu B. A review of developments in energy storage systems for hybrid excavators.
471 *Automation in Construction*. 2017, 80: 1-10. <http://dx.doi.org/10.1016/j.autcon.2017.03.010>.
- 472 [3] Ge L, Quan L, Zhang X, et al. Efficiency improvement and evaluation of electric hydraulic excavator with speed
473 and displacement variable pump. *Energy Conversion and Management*. 2017, 150: 62-71.
474 <http://dx.doi.org/10.1016/j.enconman.2017.08.010>.
- 475 [4] Axin M, Eriksson B, Krus P. Flow versus pressure control of pumps in mobile hydraulic systems. *Proceedings*
476 *of the Institution of Mechanical Engineers, Part I: Journal of Systems and Control Engineering*. 2014, 228(4): 245-256.
477 <http://dx.doi.org/10.1177/0959651813512820>.
- 478 [5] Ding R, Zhang J, Xu B, et al. Programmable hydraulic control technique in construction machinery: Status,
479 challenges and countermeasures. *Automation in Construction*. 2018, 95: 172-192.
480 <https://doi.org/10.1016/j.autcon.2018.08.001>.
- 481 [6] Lin J, Yeh T J. Mode switching control of dual-evaporator air-conditioning systems. *Energy Conversion and*
482 *Management*. 2009, 50: 1542-1555. <http://dx.doi.org/10.1016/j.enconman.2009.02.010>.
- 483 [7] Wen H, Su B. Hybrid-mode interleaved boost converter design for fuel cell electric vehicles. *Energy Conversion*
484 *and Management*. 2016, 122: 477-487. <http://dx.doi.org/10.1016/j.enconman.2016.06.021>.
- 485 [8] Wang E, Di Guo, Yang F. System design and energetic characterization of a four-wheel-driven series - parallel
486 hybrid electric powertrain for heavy-duty applications. *Energy Conversion and Management*. 2015, 106: 1264-1275.
487 <http://dx.doi.org/10.1016/j.enconman.2015.10.056>.
- 488 [9] Solouka A, Shakiba-Herfeh M, Arora J, et al. Fuel consumption assessment of an electrified powertrain with a
489 multi-mode high-efficiency engine in various levels of hybridization. *Energy Conversion and Management*. 2018, 155:
490 100-115. <http://dx.doi.org/10.1016/j.enconman.2017.10.073>.
- 491 [10] Bayomi N N, El-Maksoud R M A. Two operating modes for turbocharger system. *Energy Conversion and*
492 *Management*. 2012, 58: 59-65. <http://dx.doi.org/10.1016/j.enconman.2012.01.003>.
- 493 [11] Lin T, Chen Q, Ren H, et al. Review of boom potential energy regeneration technology for hydraulic construction
494 machinery. *Renewable and Sustainable Energy Reviews*. 2017, 79: 358-371.
495 <http://dx.doi.org/10.1016/j.rser.2017.05.131>.
- 496 [12] Liang X, Virvalo T. An energy recovery system for a hydraulic crane. *Proceedings of the Institution of*
497 *Mechanical Engineers, Part C: Journal of Mechanical Engineering Science*. 2001, 215(6): 737-744.
498 <http://dx.doi.org/10.1243/0954406011523983>.
- 499 [13] Casoli P, Gambarotta A, Pompini N, et al. Hybridization methodology based on DP algorithm for hydraulic
500 mobile machinery — Application to a middle size excavator. *Automation in Construction*. 2016, 61: 42-57.
501 <http://dx.doi.org/10.1016/j.autcon.2015.09.012>.
- 502 [14] Vukovic M, Leifeld R, Murrenhoff H. STEAM - a hydraulic hybrid architecture for excavators. *10th*
503 *International Fluid Power Conference*. Dresden, Germany: 2016.
- 504 [15] Xia L, Quan L, Ge L, et al. Energy efficiency analysis of integrated drive and energy recuperation system for
505 hydraulic excavator boom. *Energy Conversion and Management*. 2018, 156: 680-687.
506 <https://dx.doi.org/10.1016/j.enconman.2017.11.074>.

507 [16] **Ge L, Quan L, Li Y, et al.** A novel hydraulic excavator boom driving system with high efficiency and potential
508 energy regeneration capability. *Energy Conversion and Management*. 2018, 166.
509 <https://dx.doi.org/10.1016/j.enconman.2018.04.046>.

510 [17] **Kim H, Yoo S, Cho S, et al.** Hybrid control algorithm for fuel consumption of a compound hybrid excavator.
511 *Automation in Construction*. 2016, 68: 1-10. <http://dx.doi.org/10.1016/j.autcon.2016.03.017>.

512 [18] **Minav T A, Pyrhonen J J, Laurila L I E.** Permanent Magnet Synchronous Machine Sizing: Effect on the Energy
513 Efficiency of an Electro-Hydraulic Forklift. *IEEE Transactions on Industrial Electronics*. 2012, 59(6): 2466-2474.
514 <http://dx.doi.org/10.1109/TIE.2011.2148682>.

515 [19] **Minav T A, Laurila L I E, Pyrhönen J J.** Analysis of electro-hydraulic lifting system's energy efficiency with
516 direct electric drive pump control. *Automation in Construction*. 2013, 30: 144-150.
517 <http://dx.doi.org/10.1016/j.autcon.2012.11.009>.

518 [20] **Minava T A, Heikkinen J E, Pietola M.** Direct driven hydraulic drive for new powertrain topologies for non-road
519 mobile machinery. *Electric Power Systems Research*. 2017, 152: 390-400. <http://dx.doi.org/10.1016/j.epsr.2017.08.003>.

520 [21] **Eriksson B, Palmberg J.** Individual metering fluid power systems: challenges and opportunities. *Proceedings of*
521 *the Institution of Mechanical Engineers, Part I: Journal of Systems and Control*. 2011(225): 196-211.
522 <http://dx.doi.org/10.1243/09596518JSCE1111>.

523 [22] **Lu L, Yao B.** Energy-Saving Adaptive Robust Control of a Hydraulic Manipulator Using Five Cartridge Valves.
524 *IEEE Transaction on Industrial Electronics*. 2014, 61(12): 7046-7054. <https://doi.org/10.1109/TIE.2014.2314054>.

525 [23] **Choi K, Seo J, Nam Y, et al.** Energy-saving in excavators with application of independent metering valve.
526 *Journal of Mechanical Science and Technology*. 2015, 29(1): 387-395. <http://dx.doi.org/10.1007/s12206-014-1245-5>.

527 [24] **Kolks G, Weber J.** Modiciency - Efficient industrial hydraulic drives through independent metering using optimal
528 operating modes. *10th International Fluid Power Conference*. Dresden: 2016.

529 [25] **Nurmi J, Mattila J.** Global energy-optimised redundancy resolution in hydraulic manipulators using dynamic
530 programming. *Automation in Construction*. 2017, 73: 120-134. <http://dx.doi.org/10.1016/j.autcon.2016.09.006>.

531 [26] **Koivumäki J, Zhu W, Mattilaa J.** Energy-Efficient and High-Precision Control of Hydraulic Robots. *Control*
532 *Engineering Practice*. 2019. 10.1109/TIE.2014.2314054 10.1016/j.conengprac.2018.12.013.

533 [27] **Liu B, Quan L, Ge L.** Research on the performance of hydraulic excavator boom based pressure and flow
534 accordance control. *Proceedings of the Institution of Mechanical Engineers, Part E: Journal of Mechanical*
535 *Engineering*. 2017, 231(5): 901-913. <https://doi.org/10.1177/0954408916673117>.

536 [28] **Shi J, Quan L, Zhang X, et al.** Electro-hydraulic velocity and position control based on independent metering
537 valve control in mobile construction equipment. *Automation in Construction*. 2018, 94: 73-84.
538 <https://doi.org/10.1016/j.autcon.2018.06.005>.

539 [29] **Cheng M, Zhang J, Xu B, et al.** Decoupling compensation for damping improvement of the electrohydraulic
540 control system with multiple actuators. *IEEE/ASME Transactions on Mechatronics*. 2018, 23(3): 1383-1392.
541 <http://dx.doi.org/10.1109/TMECH.2018.2834936>.

542 [30] **Sheikholeslami M, Ganji D D.** Heat transfer improvement in a double pipe heat exchanger by means of
543 perforated turbulators. *Energy Conversion and Management*. 2016, 127: 112-123.
544 <http://dx.doi.org/10.1016/j.enconman.2016.08.090>.

545 [31] **Sheikholeslami M, Ganji D D.** Heat transfer enhancement in an air to water heat exchanger with discontinuous
546 helical turbulators; experimental and numerical studies. *Energy*. 2016, 116: 341-352.
547 <http://dx.doi.org/10.1016/j.energy.2016.09.120>.

548